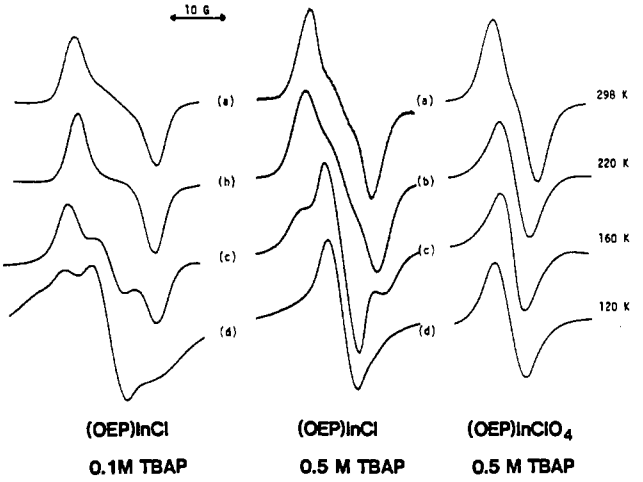

Figure 6. ESR spectra of (OEP)InCl (0.1 M TBAP), (OEP)InCl (0.5 M TBAP), and (OEP)$InClO_4$ (0.5 M TBAP) at various temperatures in CH_2Cl_2: (a) 298 K; (b) 220 K; (c) 160 K; (d) 120 K.

Table V. Coupling Constants for Different Cation Radicals of (P)M(L) and $(P)M(L)_2$

metal	axial ligand, L	a_M, G TPP	a_M, G OEP	ref[a]
Co(III)	ClO_4^-	5.7	1.2	16, 17
Zn(II)	ClO_4^-	1.22	≃0	18-20
In(III)	Cl^-	14.1	≃0	tw
	ClO_4^-	14.1	≃0	tw
Tl(III)	ClO_4^-	11.8	65.5	21
	CN^-	55.8	19.5	21

[a] tw = this work.

phenylporphyrin complexes. In contrast, the octaethylporphyrinic cation radicals $[(OEP)Mg]^{+\cdot}$ and $[(OEP)Zn]^{+\cdot}$ have optical spectra typical of an A_{1u} state and display no coupling with the metal.[18] In the present study, the same behavior is observed for the octaethylporphyrin derivatives $[(OEP)InCl]^{+\cdot}$ and $[(OEP)InClO_4]^{+\cdot}$. Indeed, the one-electron oxidation of (OEP)InCl yields radicals with a characteristic singlet ESR signal as shown in Figure 6. However, at temperatures below 200 K, the oxidized complex leads to a spectrum with two singlet ESR signals and shows a reversible temperature dependence. If the concentration of the supporting electrolyte is increased to 0.5 M TBAP and the temperature is lowered, the signal observed at room temperature disappears. This is shown in Figure 6c,d. In contrast, the oxidized $(OEP)InClO_4$ complex exhibits only one singlet in the range 293-120 K but the total width of this singlet is smaller at low temperature. The above observations clearly indicate that ESR spectra of the (OEP)InX derivatives exhibit the same line-width variations depending on the temperature and the nature of the anion of the supporting electrolyte. We, therefore, ascribe the evolution of the ESR signals to the fact that the metal interacts with the anion of the supporting electrolyte at low temperature.

Finally, it is of interest to compare the above results to those observed for other metalloporphyrin radical cations. As shown in Table V, the metal couplings depend strictly on the nature of the macrocyclic and axial ligands. For the cobalt, zinc, and indium series, the ratio of the coupling constants, $a_M(TPP)/a_M(OEP)$, demonstrates that the origin of the metal couplings arise from a $\sigma-\pi$ spin polarization mechanism while both the $\sigma-\pi$ spin polarization and direct π interaction mechanisms are involved for the thallium series.

In summary, the electrochemical, spectroelectrochemical, and ESR results are consistent with the formation of anion and cation radicals and give no evidence for the formation of discrete In(II) or In(IV) oxidation states. These data, however, do not rule out the formation of a highly oxidized or highly reduced indium atom in those metalloporphyrins containing a metal-metal or metal-carbon σ bond.

Acknowledgment. The support of the National Science Foundation (Grant CHE 8215507) is gratefully acknowledged.

Registry No. TBAP, 1923-70-2; (TPP)InCl, 63128-70-1; $[(TPP)InCl]^{2+}$, 97644-36-5; $[(TPP)InCl]^{+}$, 97644-35-4; $[(TPP)InCl]^{-}$, 97644-33-2; $[(TPP)InCl]^{2-}$, 97644-34-3; $(TPP)InClO_4$, 91312-86-6; $[(TPP)InClO_4]^{2+}$, 97644-40-1; $[(TPP)InClO_4]^{+}$, 97644-39-8; $[(TPP)InClO_4]^{-}$, 97644-37-6; $[(TPP)InClO_4]^{2-}$, 97644-38-7; (OEP)InCl, 32125-07-8; $[(OEP)InCl]^{2+}$, 97644-44-5; $[(OEP)InCl]^{+}$, 97644-43-4; $[(OEP)InCl]^{-}$, 97644-41-2; $[(OEP)InCl]^{2-}$, 97644-42-3; $(OEP)InClO_4$, 96363-81-4; $[(OEP)InClO_4]^{2+}$, 97644-48-9; $[(OEP)InClO_4]^{+}$, 97644-47-8; $[(OEP)InClO_4]^{-}$, 97644-45-6; $[(OEP)InClO_4]^{2-}$, 97644-46-7; $TBA(PF_6)$, 3109-63-5.

Contribution from the Laboratoire de Synthese et d'Electrosynthese Organometallique Associe au CNRS (LA 33), Faculte des Sciences "Gabriel", 21100 Dijon, France, and Department of Chemistry, University of Houston—University Park, Houston, Texas 77004

Reactions of σ-Bonded Alkyl- and Aryliron Porphyrins with Nitric Oxide. Synthesis and Electrochemical Characterization of Six-Coordinate Nitrosyl σ-Bonded Alkyl- and Aryliron Porphyrins

R. GUILARD,*[1a] G. LAGRANGE,[1a] A. TABARD,[1a] D. LANÇON,[1b] and K. M. KADISH*[1b]

Received February 7, 1985

The synthesis and physical characterization of 12 six-coordinate nitrosyl σ-bonded alkyl- and aryliron porphyrins were investigated in nonaqueous media. The ligands σ bonded to the nitrosyliron octaethylporphyrin or tetraphenylporphyrin complexes were CH_3, n-C_4H_9, C_6H_5, C_6H_4Me-p, C_6H_4OMe-p, and C_6F_4H. Each neutral complex was characterized by ^1H NMR, IR, and UV-visible spectroscopy, and on the basis of these data, the central metal was assigned as being in the Fe(II) oxidation state. The electrochemistry of two complexes, $(OEP)Fe(C_6H_5)(NO)$ and $(TPP)Fe(C_6H_5)(NO)$, was carried out, and results of this study were evaluated with respect to the spectroscopic characterization of the complexes. Finally, comparisons were made between the reactivities and physicochemical properties of the investigated six-coordinate complexes and other related iron σ-bonded alkyl and iron nitrosyl complexes in the literature.

Introduction

Studies on the binding and activation of small molecules by metalloporphyrins are of major interest due to the potential importance of these reactions in catalytic processes involving biological reactions.[2-5] Evidence has been provided for the formation

(1) (a) University of Dijon. (b) University of Houston.

(2) Dolphin, D. Ed. "The Porphyrins"; Academic Press: New York, 1979; Vol. I-VII.

(3) Buchler, J. W. *Angew. Chem., Int. Ed. Engl.* **1978**, *17*, 407.

0020-1669/85/1324-3649$01.50/0

Table I. Notation Utilized for the Various (OEP)Fe(R)(NO) and (TPP)Fe(R)(NO) Complexes

ligand notation	R group	porphyrin ligand OEP, 1	porphyrin ligand TPP, 2
a	CH_3	**1a**	**2a**
b	n-C_4H_9	**1b**	**2b**
c	C_6H_5	**1c**	**2c**
d	C_6H_4Me-p	**1d**	**2d**
e	C_6H_4OMe-p	**1e**	**2e**
f	C_6F_4H	**1f**	**2f**

of a nitric oxide–hemoglobin complex,[6-8] and numerous reactions can be initiated by nitrosylhemoglobin. More specifically, the nitrosation of amines leading to cancerogenic nitrosamines has been clearly established.[9]

Studies of synthetic iron porphyrins that are σ-bonded with alkyl or aryl groups are also of great interest. During the past decade studies of substrate activation by cytochrome P450 have revealed the formation of σ-bonded alkyl- or aryliron(III) P450 complexes,[10-13] and this has naturally initiated a considerable amount of research on synthetic iron σ-bonded porphyrins.[14-20]

The above biological implications led us to investigate the possibility of synthesizing σ-bonded alkyl- and aryliron porphyrins that are also bound with nitric oxide as a sixth axial ligand. These syntheses were possible, and in two preliminary notes we reported the partial characterization[21] and electrochemistry[22] of the first synthetic iron σ-bonded metalloporphyrins containing a bound NO ligand. We have now extended this study to a number of octaethylporphyrin and tetraphenylporphyrin σ-bonded NO complexes whose complete synthesis and physicochemical characterization are given in this paper. A list of the specific compounds and the notation utilized for them in this paper are given in Table I.

Experimental Section

Chemicals. (TPP)Fe^{II}(NO) and (OEP)Fe^{II}(NO) were synthesized from (TPP)Fe^{III}Cl or (OEP)Fe^{III}Cl by literature methods.[23-26] Nitric oxide gas was purchased from Matheson Gas products (for the synthetic work) or from Union Carbide Co. (for the electrochemical measurements). This gas was passed through KOH pellets prior to use. The synthesis and handling of the metalloporphyrins were carried out under an atmosphere of argon. All common solvents were thoroughly dried in an appropriate manner and were distilled under argon prior to use. All operations were carried out in Schlenk tubes under purified argon and with dried oxygen-free solvents. The supporting electrolyte used for the electrochemistry was the tetra-n-butylammonium salt of hexafluorophosphate (TBA(PF_6)), which was obtained from Eastman Chemicals or Fluka Chemical Co. This inert salt was recrystallized from ethanol and dried in vacuo at 100 °C before storage in a desiccator.

The five-coordinate σ-bonded alkyl- and aryliron porphyrins (OEP)Fe(R) and (TPP)Fe(R), where R = alkyl, aryl, were prepared according to literature methods.[18,19,27] The six-coordinate (TPP)Fe(R)(NO) and (OEP)Fe(R)(NO) complexes were synthesized by the reaction of nitric oxide with the corresponding (OEP)Fe(R) or (TPP)Fe(R) complex. Formation of the six-coordinate complex could be accomplished by the exposure of degassed solid (TPP)Fe(R) or (OEP)Fe(R) to 1 atm of nitric oxide or, alternatively, by exposing solutions of 5×10^{-3} M (P)Fe(R) in toluene saturated with argon to 1 atm of nitric oxide. The elemental analysis and mass spectral data of the synthesized complexes are summarized in Table II. Elemental analyses were performed by the "Service de Microanalyses du CNRS".

Instrumentation. Mass spectra were recorded in the electron-impact mode: ionizing energy 30–70 eV; ionizing current 0.4 mA; source temperature 250–400 °C. ^{1}H NMR spectra were recorded on a JEOL FX 100 spectrometer. Spectra were measured for (P)Fe(R)(NO) solutions in 0.5 mL of C_6D_6 with tetramethylsilane as internal reference. Accumulations of 20–200 scans over 16K points were made for each spectrum at 21 ± 1 °C. Infrared spectra were achieved on a Perkin-Elmer 580B instrument. Samples were 1% dispersions in Nujol mulls. Electronic absorption spectra were performed on a Perkin-Elmer 559 spectrophotometer using 5×10^{-3} M solutions of (P)Fe(R)(NO) in toluene.

Cyclic voltammetric measurements were obtained with one of three different experimental setups. For experiments at a potential scan rate lower than 0.30 V/s, a PAR Model 174A polarographic analyzer, an IBM Instruments Model EC225 voltammetric analyzer, or a Bioanalytical Systems (BAS) Model CV-1B were used in conjunction with a Houston Instruments Model 2000 XY recorder. Scan rates higher than 0.30 V/s required a PAR Model 173/176 potentiostat/galvanostat and a PAR Model 178 electronic probe driven by a PAR Model 175 universal programmer, or an IBM Instruments Model EC225 voltammetric analyzer. Current–voltage curves taken at sweep rates between 0.30 and 20.0 V/s were recorded on a Tektronix Model 5111 storage oscilloscope with a Tektronix Model C5-A camera attachment. A three-electrode configuration was used for all cyclic voltammetry experiments. This consisted of a platinum-button working electrode and an IBM saturated calomel electrode (SCE) as the reference electrode. Typically, the utilized electrochemical Brinkman Model EA-875 cells needed 5–10-mL solution volumes.

Differential pulse polarography (DPP) was obtained with a PAR Model 174A polarographic analyzer or an IBM Instruments Model EC225 voltammetric analyzer, in conjunction with a Houston Instruments Model 2000 XY recorder. A DME or platinum-button electrode served as the working electrode. Typically, instrument settings included a potential scan rate of 0.005 V/s, a pulse width of 0.5 s, and a potential pulse of 25 mV.

A vacuum-tight cell was utilized for experiments conducted under a controlled atmosphere (inert gas or nitric oxide). This cell was also utilized for controlled-potential electrolysis. Its design was such that electronic absorption spectra could be acquired via an attached spectrophotometric cell. The attached spectrophotometric cell had a 0.2-cm path length, and the overall minimum solution was 10 mL. Finally, all potentials were reported vs. a saturated calomel electrode and are good to ±0.01 V.

Results and Discussion

Synthesis of (OEP)Fe(R)(NO) and (TPP)Fe(R)(NO). The σ-bonded alkyl- or aryliron porphyrins react quickly with nitric oxide to form the (OEP)Fe(R)(NO) and (TPP)Fe(R)(NO) de-

(4) (a) Collman, J. P.; Brauman, J. J.; Docsee, K. M. *Proc. Natl. Acad. Sci. U.S.A.* **1979**, *79*, 6035. (b) Collman, J. P.; Denisevich, P.; Konai, Y.; Marocco, M.; Koval, C.; Anson, F. C. *J. Am. Chem. Soc.* **1980**, *102*, 6027.
(5) Drago, R. S.; Corden, B. B. *Acc. Chem. Res.* **1980**, *13*, 353.
(6) Oda, H.; Nogami, H.; Kusumoto, S.; Nakajima, T.; Kurata, A.; Imai, K. *Bull. Environ. Contam. Toxicol.* **1976**, *16*, 582.
(7) Freeman, G.; Dyer, R. L.; Juhos, L. T.; St. John, G. A.; Anbar, M. *Arch. Environ. Health* **1978**, *33*, 19.
(8) Gibson, Q. H.; Roughton, F. J. W. *J. Physiol. (London)* **1957**, *136*, 507.
(9) Bonnett, H. R.; Charalambides, A. A.; Martin, R. A.; Sales, K. D.; Fritzsimmons, B. W. *J. Chem. Soc., Chem. Commun.* **1975**, 884.
(10) Uehleke, H.; Hellmer, K. H.; Tabarelli-Poplawski, S. *Arch. Pharm. (Weinheim, Ger.)* **1973**, *279*, 39.
(11) Mansuy, D.; Nastainczyk, W.; Ullrich, V. *Arch. Pharm. (Weinheim, Ger.)* **1974**, *285*, 315.
(12) Wolf, C. R.; Mansuy, D.; Nastainczyk, W.; Deutschmann, G.; Ullrich, V. *Mol. Pharmacol.* **1977**, *13*, 698.
(13) (a) Ortiz de Montellano, P. R.; Kunze, K. L. *J. Am. Chem. Soc.* **1981**, *103*, 6534. (b) Augusto, O.; Kunze, K. L.; Ortiz de Montellano, P. R. *J. Biol. Chem.* **1982**, *257*, 6231.
(14) Lexa, D.; Saveant, J. M.; Battioni, J. P.; Lange, M.; Mansuy, D. *Angew. Chem., Int. Ed. Engl.* **1981**, *20*, 578.
(15) Lexa, D.; Mispelter, J.; Saveant, J. M. *J. Am. Chem. Soc.* **1981**, *103*, 6806.
(16) Brault, D.; Neta, P. *J. Phys. Chem.* **1982**, *86*, 3405.
(17) Lexa, D.; Saveant, J. M. *J. Am. Chem. Soc.* **1982**, *104*, 3503.
(18) Cocolios, P.; Laviron, E.; Guilard, R. *J. Organomet. Chem.* **1982**, *228*, C39.
(19) Cocolios, P.; Lagrange, G.; Guilard, R. *J. Organomet. Chem.* **1983**, *253*, 65.
(20) Ogoshi, H.; Sugimoto, H.; Yoshida, Z.; Kobayashi, H.; Sakai, H.; Maeda, Y. *J. Organomet. Chem.* **1982**, *234*, 185.
(21) Lagrange, G.; Cocolios, P.; Guilard, R. *J. Organomet. Chem.* **1984**, *260*, C16.
(22) Kadish, K. M.; Lançon, D.; Cocolios, P.; Guilard, R. *Inorg. Chem.* **1984**, *23*, 2372.
(23) Wayland, B. B.; Olson, L. W. *J. Am. Chem. Soc.* **1974**, *96*, 6037.
(24) Scheidt, W. R.; Frisse, M. E. *J. Am. Chem. Soc.* **1975**, *97*, 2517.
(25) Buchler, J. W.; Lay, K. L. *Z. Naturforsch., B: Anorg. Chem., Org. Chem.* **1975**, *30B*, 385.
(26) Spaulding, L. D.; Chang, C. C.; Yu, N. T.; Felton, R. H. *J. Am. Chem. Soc.* **1975**, *97*, 2517.
(27) Guilard, R.; Boisselier-Cocolios, B.; Tabard, A.; Cocolios, P.; Simonet, B.; Kadish, K. M. *Inorg. Chem.* **1985**, *24*, 2509.

Table II. Elemental Analysis and Mass Spectral Data of the Pure (P)Fe(R)(NO) Complexes

complex	anal. found (calcd) % C	% H	% N	% F	% Fe	*m/e*	rel intens	frag pattern
(OEP)Fe(C_6H_5)(NO) (**1c**)	72.5	7.1	9.8		8.0	665	33.2	[(OEP)Fe(C_6H_5)]$^+$·
	(72.50)	(7.11)	(10.06)		(8.03)	588	100	[(OEP)Fe]$^+$
(OEP)Fe(C_6H_4OMe-*p*)(NO) (**1e**)	71.1	7.1	10.0		8.0	696	13.2	[(OEP)Fe(C_6H_4OMe-*p*)]$^+$·
	(71.16)	(7.09)	(9.64)		(7.69)	588	100	[(OEP)Fe]$^+$
(TPP)Fe(C_6H_5)(NO) (**2c**)	77.0	4.3	8.7		7.4	746	28.5	[(TPP)Fe(C_6H_5)]$^+$·
	(77.41)	(4.29)	(9.02)		(7.20)	668	100	[(TPP)Fe]$^+$
						667	30.6	[(TPP)Fe-H]$^+$·
(TPP)Fe(C_6H_4Me-*p*)(NO) (**2d**)	77.2	4.5	8.1		7.0	759	30.2	[(TPP)Fe(C_6H_4Me-*p*)]$^+$·
	(77.56)	(4.47)	(8.86)		(7.07)	668	100	[(TPP)Fe]$^+$
(TPP)Fe(C_6H_4OMe-*p*)(NO) (**2e**)	75.9	4.6	8.4		6.5	805	0.7	[(TPP)Fe(C_6H_4OMe-*p*)(NO)]$^+$·
	(76.03)	(4.38)	(8.69)		(6.93)	774	44.3	[(TPP)Fe(C_6H_4OMe-*p*)]$^+$·
						668	100	[(TPP)Fe]$^+$
(TPP)Fe(C_6F_4H)(NO) (**2f**)	69.5	3.5	7.4	7.6	6.4	848	0.5	[(TPP)Fe(C_6F_4H)(NO)]$^+$·
	(70.84)	(3.45)	(8.26)	(8.96)	(6.59)	818	100	[(TPP)Fe(C_6F_4H)]$^+$·

rivatives. However, for some complexes displacement of the R group occurred and the known five-coordinate (TPP)Fe(NO) or (OEP)Fe(NO) species was produced. This is shown by reaction 1. No evidence for dinitrosyl formation was present in the solid

$$\text{(P)Fe(R)} \xrightarrow{\text{NO}} \text{(P)Fe(R)(NO)} + \text{(P)Fe(NO)} \qquad (1)$$

state although, in solutions containing TBA(PF_6), some dinitrosyl complexes as well as another unstable intermediate could be formed. The nature of this intermediate is discussed in later sections.

The relative proportions of obtained (P)Fe(R)(NO) and (P)-Fe(NO) depended on the nature of the axial and the equatorial (porphyrinic) ligands. The aryliron complexes of NO with OEP ligands (compounds **1c–f**) and TPP ligands (compounds **2c–f**) were obtained in close to 100% yield without trace of the five-coordinate nitrosyl derivatives. In addition, the TPP complexes were generally more stable than the OEP derivatives and were obtained in slightly higher purity. This difference in stability between the derivatives with different porphyrin ligands was also observed for the four complexes containing σ-bonded alkyl groups (compounds **1a,b**, **2a,b**), and with these ligands, the reaction with NO always led to a mixture as shown in reaction 1. For the methyliron compounds, (P)Fe(CH_3)(NO) and (P)Fe(NO) were formed in approximately equal parts. On the other hand, when R = *n*-C_4H_9 only traces of (P)Fe(*n*-C_4H_9)(NO) were detected, the major product being (P)Fe(NO). These mixtures are not noted in Table II, which reports elemental analysis and mass spectral data only for the pure (P)Fe(R)(NO) derivatives.

The formation of (OEP)Fe(R)(NO) and (TPP)Fe(R)(NO) from (OEP)Fe(R) or (TPP)Fe(R) was also possible in solution. However, when nitric oxide was allowed to slowly diffuse into a toluene solution of the σ-bonded alkyl- or aryliron porphyrin, the reaction gave a mixture of three products. Two of these were identified as the products of reaction 1, i.e., (P)Fe(R)(NO) and (P)Fe(NO), while the third species was an unstable intermediate that could not be isolated. The actual proportion of the reaction products for a given OEP or TPP complex depended on the nature of the axial and equatorial ligands as well as the concentration of nitric oxide in the toluene solution. Generally, high concentrations of NO gave lower yields of the six-coordinate (P)Fe-(R)(NO) species.

The structures of the synthesized (P)Fe(R)(NO) complexes were established on the basis of various spectrochemical data. Mass spectral data for six of the most stable (P)Fe(R)(NO) complexes with bound aryl groups appear in Table II. For five of the six complexes (compounds **1c,e**, **2c–e**) the base peak corresponded to the ionic species, [(P)Fe]$^+$. The σ-bonded [(P)-Fe(R)]$^+$· ions also showed significant intensity (10–50%), and for (TPP)Fe(C_6F_4H)(NO) (compound **2f**), the [(P)Fe(R)]$^+$· ion corresponded to the base peak. Finally, only (TPP)Fe-(C_6H_4OMe-*p*)(NO) (compound **2e**) and (TPP)Fe(C_6F_4H)(NO) (compound **2f**) had parent peaks corresponding to the stable nitrosyl complex. These molecular peaks of [(P)Fe(R)(NO)]$^+$· were quite weak for both complexes, consistent with the easy loss of nitric oxide. This is not surprising since the labile character of the metal–NO bond is well established.[28] In addition, all the mass spectral observations are in good agreement with nitric oxide binding either cis or trans to the alkyl or aryl group.

Table III. IR Stretching Frequencies (ν_{NO}, cm^{-1}) of NO Bound as (P)Fe(R)(NO) or (P)Fe(NO)

R group	porphyrin ligand OEP	TPP	R group	porphyrin ligand OEP	TPP
none[a]	1670	1698.8	C_6H_4Me-*p*	1785.4	1792
CH_3	1766	1789	C_6H_4OMe-*p*	1790.5	1803.3
n-C_4H_9		1764	C_6F_4H	1838.8	1850
C_6H_5	1795	1790.5			

[a] Stretching frequencies are of (OEP)Fe(NO) and (TPP)Fe(NO), respectively.

Spectroscopic Characterization of (P)Fe(R)(NO). Infrared spectroscopy is a powerful method to study complexes with bound nitric oxide since the ν_{NO} stretching frequency is strictly dependent on the M–N–O bond angle.[29] For the mononitrosyl complexes, (TPP)Fe(NO) and (OEP)Fe(NO), the observed NO stretching frequencies are 1670 and 1698.8 cm^{-1}, respectively. This latter value is in agreement with a ν_{NO} of 1700 cm^{-1} reported by Wayland and Olson[30] for (TPP)Fe(NO) in a Nujol mull and is consistent with a bent Fe–NO^- unit. In contrast, the dinitrosyl Fe(II) complex (TPP)Fe($NO)_2$ has ν_{NO} stretching frequencies at 1870 and 1690 cm^{-1} and may be associated with one linear Fe–NO^+ unit (1870 cm^{-1}) and one bent Fe–NO^- unit (1690 cm^{-1}).

Values of ν_{NO} for each of the (P)Fe(R)(NO) complexes are given in Table III and range between 1764 and 1850 cm^{-1} depending upon the nature of the porphyrin ligand and the specific bound aryl or alkyl group. Generally, for a given R group, the values of ν_{NO} are larger for the TPP derivatives than for the OEP derivatives. This is also true for the mononitrosyl complex without the σ-bonded alkyl or aryl ligand and has been observed for other nitrosyl porphyrins with different central metals.[28]

The values of ν_{NO} for (P)Fe(R)(NO) are typical of a terminal nitrosyl, which is generally observed in the range 1650–1900 cm^{-1}.[29] In addition, the IR data of the (P)Fe(R)(NO) complexes range between values expected for linear Fe–NO^+ (1800–1900 cm^{-1}) and bent Fe–NO^- ($\leq$1700 cm^{-1}) units.[30]

It has been shown by Scheidt[31,32] that a linear correlation exists between the Fe–N_b bond distance and the ν_{NO} stretching frequencies of six-coordinate nitrosyliron porphyrins (for this cor-

(28) Wayland, B. B.; Newman, A. R. *Inorg. Chem.* **1981**, *20*, 3093.
(29) (a) Nakamoto, K. "Infrared and Raman Spectra of Inorganic Coordination Compounds", 3rd ed.; Wiley: New York, 1978; (b) Cotton, F. A.; Wilkinson, G. "Advanced Inorganic Chemistry"; Wiley-Interscience: New York, 1980.
(30) Wayland, B. B.; Olson, L. W. *J. Am. Chem. Soc.* **1974**, *96*, 6037.
(31) Scheidt, W. R.; Picuilo, P. L. *J. Am. Chem. Soc.* **1976**, *98*, 1913.
(32) Scheidt, W. R.; Brinegar, A. C.; Ferro, E. B.; Kirner, J. F. *J. Am. Chem. Soc.* **1977**, *99*, 7315.

Table IV. ^{1}H NMR Data[a] of the (P)Fe(R)(NO) Complexes

complex	R^1	R^2	R(Ar)	protons of R^1	m/*i*[b]	δ	protons of R^2	m/*i*	δ	protons of R(Ar)	m/*i*	δ
(OEP)Fe(C_6H_5)(NO) (**1c**)	H	CH_2CH_3	C_6H_5		s/4	10.12	CH_2	q/16	3.85	*p*-H	m/1	4.95
							CH_3	t/24	1.81	*o,m*-H	m/4	4.68
(OEP)Fe(C_6H_4Me-*p*)(NO) (**1d**)	H	CH_2CH_3	C_6H_4Me-*p*		s/4	10.11	CH_2	q/16	3.88	*p*-Me	s/3	0.56
							CH_3	t/24	1.84	*o,m*-H	m/4	4.45
(OEP)Fe(C_6H_4OMe-*p*)(NO) (**1e**)	H	CH_2CH_3	C_6H_4OMe-*p*		s/4	10.14	CH_2	q/16	3.89	*p*-OMe	s/3	2.10
							CH_3	t/24	1.86	*o,m*-H	m/4	4.25
(OEP)Fe(C_6F_4H)(NO) (**1f**)	H	CH_2CH_3	C_6F_4H		s/4	9.95	CH_2	8/16	3.48	*c*		
							CH_3	t/24	1.59			
(TPP)Fe(C_6H_5)(NO) (**2c**)	C_6H_5	H	C_6H_5	*o,o'*-H	d/8	8.01		s/8	8.91	*p*-H	m/1	5.43–5.29
						7.93						
				m,p-H	s/12	7.37				*o,m*-H	m/4	5.14–4.97
(TPP)Fe(C_6H_4Me-*p*)(NO) (**2d**)	C_6H_5	H	C_6H_4Me-*p*	*o,o'*-H	d/8	8.01		s/8	8.94	*p*-Me	s/3	0.98
						7.96				*o,o'*-H	m/2	4.87
				m,p-H	s/12	7.37				*m,m'*-H	m/2	4.80
(TPP)Fe(C_6H_5OMe-*p*)(NO) (**2e**)	C_6H_5	H	C_6H_4OMe-*p*	*o,o'*-H	d/8	8.01		s/8	8.91	*p*-OMe	s/3	2.33
						7.96				*o,o'*-H	m/2	4.68
				m,p-H	s/12	7.37				*m,m'*-H	m/2	4.59
(TPP)Fe(C_6F_4H)(NO) (**2f**)	C_6H_5	H	C_6F_4H	*o,o'*-H	d/8	8.01		s/8	8.94	*c*		
						7.96						
				m,p-H	s/12	7.37						

[a] Spectra recorded in C_6D_6 at 25 °C with $SiMe_4$ as internal reference; chemical shifts downfield from $SiMe_4$ are defined as positive. [b] Abbreviations: m/*i* = multiplicity/intensity, s = singlet, t = triplet, m = multiplet, q = quartet. [c] Not observed.

Table V. UV–Visible Spectroscopic Data of (TPP)Fe(R)(NO) Complexes in Toluene

complex	λ_{max}, nm ($10^{-3}\epsilon$)			
	B(1,0)	B(0,0) Soret	Q(1,0)	Q(0,0)
(TPP)Fe(CH_3)(NO) (**2a**)	332 (37.1)	430 (143.3)	541 (9.3)	579 (3.4)
(TPP)Fe(C_6H_5)(NO) (**2c**)	337 (40.3)	436 (97.7)	558 (7.6)	597 (4.3)
(TPP)Fe(C_6H_4Me-*p*)(NO) (**2d**)	338 (46.8)	436 (115.0)	556 (9.1)	597 (5.5)
(TPP)Fe(C_6H_4OMe-*p*)(NO) (**2e**)	320 (53.8)	430.5 (163.3)	543 (10.5)	580 (4.8)
(TPP)Fe(C_6F_4H)(NO) (**2f**)	328 (45.9)	431 (110.4)	550 (8.3)	604 (3.8)

relation Fe–N_b is the bond length between the iron atom and the nitrogen atom of the sixth nitrogeneous ligand). The out-of-plane displacement of the iron atom increases with decreasing interaction of the trans ligand. This thus corresponds to larger values of the Fe–N_b distance. In this manner, the pentacoordinate (TPP)Fe(NO) complex with a bent Fe–NO^- unit may be viewed as the extreme case where there is no interaction with a trans nitrogeneous ligand. Clearly, the trans binding of a nitrogenous base to nitric oxide complexes of iron porphyrins increases the ionic character of the NO, leading to a more bent Fe–NO^- unit.

The ν_{NO} frequencies of (P)Fe(R)(NO) correlate well with the electron donor properties of the alkyl or aryl group; the more electron donating the R group, the lower the ν_{NO} stretching frequency. At one extreme, the 1850-cm^{-1} ν_{NO} frequency of (TPP)Fe(C_6F_4H)(NO) is close to the ν_{NO} frequency of 1880 cm^{-1} for (TPP)Fe(Cl)(NO).[30] In this latter compound the nitrosyl group has a cationic character and consequently a linear Fe–NO^+ arrangement.

The above results on (TPP)Fe(Cl)(NO) tend to suggest that NO is bound trans to the alkyl (aryl) group in (P)Fe(R)(NO). These data also show that the bound NO is linear in (TPP)Fe(C_6F_4H)(NO) but that, with the increasing electron-donor character of the R group, a bent arrangement is induced. In this extreme, the smallest Fe–N–O angle must be logically observed for the (P)Fe(C_6F_4H)(NO) complexes where stretching frequencies of 1838.8 and 1850 cm^{-1} are observed.

^{1}H NMR measurements were carried out on the series of (OEP)Fe(R)(NO) and (TPP)Fe(R)(NO) in order to clearly establish the structure of these compounds and, at the same time, to better define the iron oxidation state. Data from these measurements are summarized in Table IV, and the notations for R^1 and R^2 are given in Figure 1. As seen in this table, the morphology of the signals and the chemical shifts of the macrocyclic protons are typical of diamagnetic species.[33] Indeed, the meso,

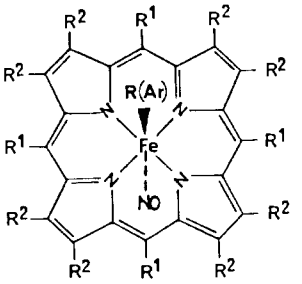

Figure 1. Schematic illustration of (P)Fe(R)(NO). The nature of the substituents R^1 and R^2 is shown in Table IV.

methylenic, and methyl protons of the octaethylporphyrin complexes appear close to 10.0, 3.8, and 1.8 ppm, respectively. For these complexes, the protons of the aryl group bound to the iron atom exhibit a signal in the region of 4.4–5.4 ppm, while the methyl or the methoxy protons of the substituted aryl group are observed between 0.5 and 2.4 ppm.

For the (TPP)Fe(R)(NO) derivatives, the pyrrolic protons show a singlet close to 8.9 ppm while the phenyl protons display three separate signals in the range 7.3–8.1 ppm. Moreover, the protons of the bound axial ligand are more deshielded than in the octaethylporphyrin series, in good agreement with the electron-donating properties and the magnetic anisotropy of this macrocycle compared to that of tetraphenylporphyrin ($\Delta\delta \simeq 0.5$). In summary, all of these results prove that the (P)Fe(R)(NO) complexes are diamagnetic. These data are also in good agreement with nitric oxide binding trans to the alkyl or aryl group in the (P)Fe(R)(NO) complexes since the anisotropy of the macrocyclic signals is very low (for example, a quadruplet is observed for the methylenic protons of the octaethylporphyrin series). This clearly establishes the binding of nitric oxide trans to the alkyl or aryl group in the (P)Fe(R)(NO) complexes.

Electronic absorption spectra of stable (TPP)Fe(R)(NO) complexes were measured in toluene, and values of maximum wavelengths and molar absorptivities are given in Table V. The

(33) Scheer, H.; Katz, J. J. In "Porphyrins and Metalloporphyrins"; Smith, K. M., Ed.; Elsevier: Amsterdam, 1975; 399.

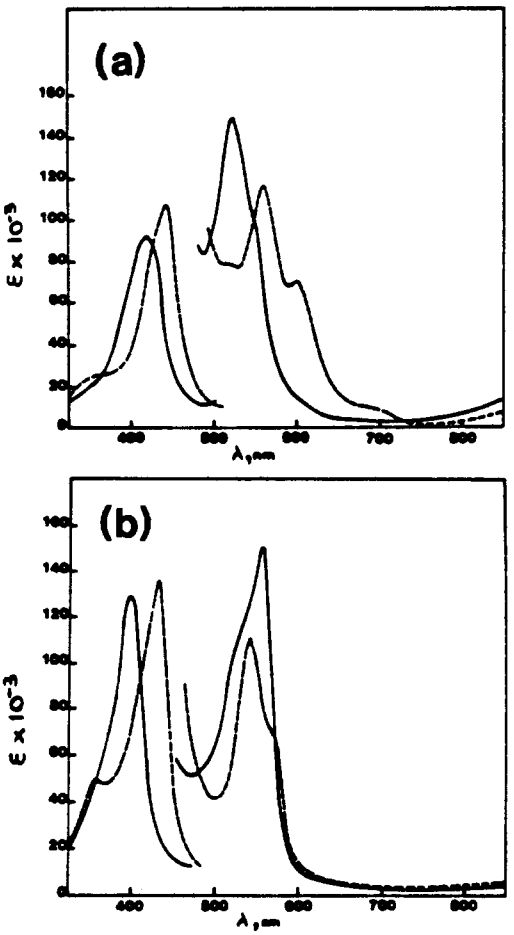

Figure 2. Electronic absorption spectra of (a) 4.94×10^{-5} M (TPP)Fe(C_6H_5) (—) and (TPP)Fe(C_6H_5)(NO) (---) under 7 mm of NO and (b) 2.80×10^{-5} M (OEP)Fe(C_6H_5) (—) and (OEP)Fe(C_6H_5)(NO) (---) under 8 mm of NO. Both sets of spectra were recorded in PhCN (0.1 M TBA(PF_6)).

Soret band is located in the region 430–436 nm, and two visible bands are observed in the region 541–604 nm. These latter values are quite close to bands for low-spin Fe(II), which are expected to be in the region 550–590 nm.[34] Consequently, the molecular orbital scheme proposed by Wayland and Olson for (TPP)Fe(Cl)(NO)[30] can also be applied to the (P)Fe(R)(NO) derivatives. For the former complexes the interaction of NO with the Fe(II) site results in an internal electron transfer from the NO π^* orbital to one of the lower energy d orbitals of the metal.

Similar electronic absorption spectra were obtained for (TPP)Fe(C_6H_5)(NO) in toluene and in PhCN containing 0.1 M TBA(PF_6) as inert supporting electrolyte. This is shown in Figure 2. Also shown in this figure are the spectra of (OEP)Fe(C_6H_5)(NO),[35] as well as (TPP)Fe(C_6H_5) and (OEP)Fe(C_6H_5) in the absence of NO gas. The spectral properties of these latter Fe(III) complexes in PhCN have been described in the literature.[36] For the case of (TPP)Fe(C_6H_5), major absorption peaks are located at 412 and 522 nm while shoulders on peaks are located at 398 and 541 nm. (OEP)Fe(C_6H_5) has two major absorption peaks located at 393 and 554 nm. A shoulder is found at 527 nm. These spectra are illustrated by the solid lines in Figure 2.

Complete conversion of (P)Fe(C_6H_5) to (P)Fe(C_6H_5)(NO) in PhCN (0.1 M TBA(PF_6)) could be accomplished under 7–8 mm NO pressure for the spectroscopic conditions of low (P)Fe(C_6H_5) concentrations. This is shown in Figure 2, where (TPP)Fe(C_6H_5)(NO) and (OEP)Fe(C_6H_5)(NO) are represented by dashed lines. As seen in this figure, the spectra of (P)Fe(R)(NO) are quite different from those of (P)Fe(R). Under the given experimental conditions, there was no evidence for significant (spectroscopically detectable) formation of either (P)Fe(NO) or (P)Fe($NO)_2$ in solution. The mono- and dinitrosyl adducts of (TPP)Fe^{II} have Soret bands at 410 and 433 nm, respectively.[37] For the case of (OEP)Fe(NO) and (OEP)Fe($NO)_2$, the Soret bands are located at 394 and 415 nm, respectively.[37] Both series of compounds are characterized as containing an Fe(II) central metal. This is also the case for (P)Fe(C_6H_5)(NO), where the spectroscopic characterization indicates an Fe(II) formulation.

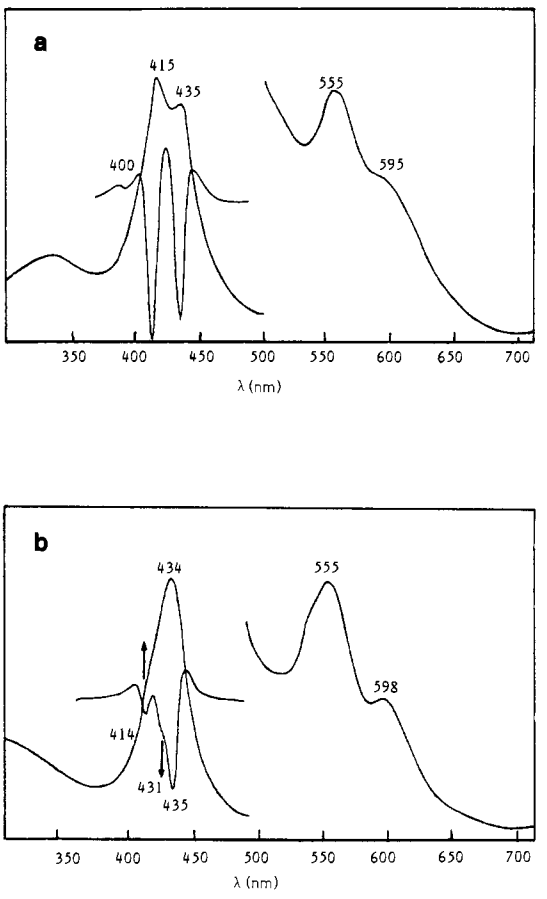

Figure 3. Electronic absorption spectra of (a) (TPP)Fe(C_6H_5)(NO) (**2c**) in toluene saturated with argon and (b) the same compound in toluene under nitric oxide. The Soret bands for identified complexes are as follows: (TPP)Fe(NO), 400 nm; intermediate, 415 nm; (TPP)Fe($NO)_2$, 431 nm; (TPP)Fe(C_6H_5)(NO), 435 nm.

Identification of the Intermediate in the Reaction of (P)Fe(R) with NO in Solution. No evidence of an intermediate species was detected in the titration of (P)Fe(C_6H_5) with NO in PhCN containing 0.1 M TBA(PF_6), nor was an intermediate observed in the conversion of solid (P)Fe(C_6H_5) to (P)Fe(C_6H_5)(NO) under an NO atmosphere. This was not the case for NO titrations of (P)Fe(C_6H_5) in toluene.

Alternative bubbling of nitric oxide and argon gas into toluene solutions of (TPP)Fe(C_6H_5)(NO) gave the UV–visible spectra shown in Figure 3. The Soret band of Figure 3a (a toluene solution of (TPP)Fe(C_6H_5)(NO) under argon) is located at 435 and 415 nm, indicating the presence of both (TPP)Fe(C_6H_5)(NO) and the unknown complex. A trace of (TPP)Fe(NO) is also suggested by the peak at 400 nm. Addition of nitric oxide to this solution led to the spectrum shown in Figure 3b. In this figure, the Soret band is located at 435 nm and is of the same intensity. However, a new band has appeared at 431 nm while the absorption of the unknown species at 415 nm has decreased. This evolution

(34) Gouterman, M. In "The Porphyrins"; Dolphin, D., Ed.; Academic Press: New York, 1978; Vol. III, Chapter I, and reference therein.
(35) A similar figure is illustrated in ref 22, but unfortunately, in this reference the legends have been incorrectly reversed.
(36) Lançon, D.; Cocolios, P.; Guilard, R.; Kadish, K. M. *J. Am. Chem. Soc.* **1984**, *106*, 4472.
(37) Lançon, D.; Kadish, K. M. *J. Am. Chem. Soc.* **1983**, *105*, 5610.

Table VI. Half-Wave or Peak Potentials (V vs. SCE) for Oxidation and Reduction of Several Iron Porphyrins Containing an Iron–Phenyl and an Iron–Nitrosyl Bond[f]

species	Fe(III) oxidn		Fe(III)/Fe(II)		Fe(II) redn	
	P = TPP	P = OEP	P = TPP	P = OEP	P = TPP	P = OEP
(P)Fe(C_6H_5)(NO)			0.86	0.73	−0.92[d]	−1.16[d]
(P)Fe(NO)[a]			0.75	0.69	−0.88	−1.08
(P)Fe$(NO)_2$[a]			0.75	0.95[e]		
(P)Fe(C_6H_5)[b]	0.61	0.48	−0.70	−0.93	>−1.90	>−1.90
(P)Fe(C_6H_5)(py)[c]	0.63	0.44	−0.76	−1.03	>−1.90	>−1.90

[a] Taken from ref 37. [b] Taken from ref 36. [c] Taken from ref 38. Data reported were measured in neat pyridine containing 0.1 M TBA(PF_6). [d] Potential quoted is peak potential measured by DPP at 5 mV/s. [e] Potential quoted is E_{pa} by cyclic voltammetry at 0.10 V/s. [f] Except where noted, all potentials are reported in PhCN (0.1 M TBA(PF_6)).

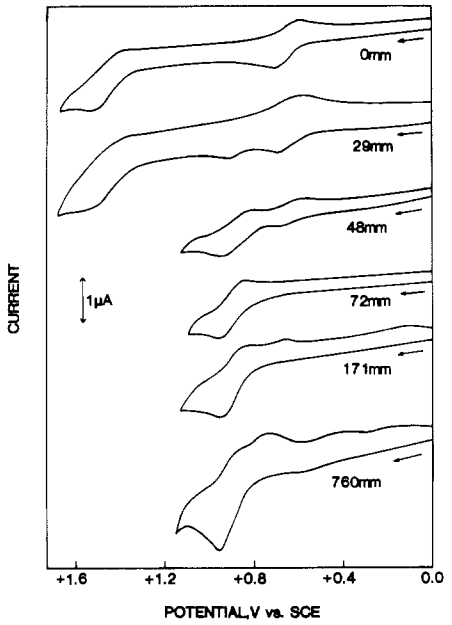

Figure 4. Cyclic voltammograms of 1.09×10^{-3} M (TPP)Fe(C_6H_5) in PhCN (0.1 M TBA(PF_6)) under various NO pressures.

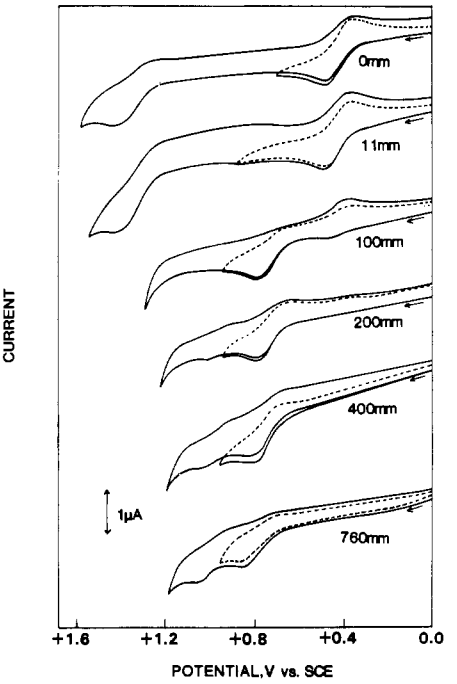

Figure 5. Cyclic voltammograms of 1.31×10^{-3} M (OEP)Fe(C_6H_5) in PhCN (0.1 M TBA(PF_6)) under various NO pressures.

of the UV–visible spectra as a function of NO pressure proves that there is no equilibrium occurring between (TPP)Fe(C_6H_5) and the unidentified species.

It is significant to note that the same intermediate was identified (but not isolated) in the conversion of (TPP)Fe(NO) to (TPP)-Fe$(NO)_2$ in toluene.[37] The intermediate, which was only present at low NO pressures, had electrochemistry similar to that of (TPP)Fe(NO) and (TPP)Fe$(NO)_2$ and was characterized by two main absorption bands at 415 and 513 nm and two smaller bands at 662 and 690 nm. On the basis of these UV–visible data, especially in the region 600–700 nm, this intermediate was postulated as an Fe(III) high-spin complex.[37]

The results of our spectroscopic studies on (P)Fe(R) and (P)Fe(NO)[37] suggest that the intermediate is formed by the reaction of NO with (P)Fe(NO). All attempts to isolate the intermediate compound have been unsuccessful. However, the ^1H NMR spectrum of the mixture resulting from addition of NO to toluene solutions of (TPP)Fe(C_6H_5) is of interest. The resulting NMR spectrum in C_6D_6 exhibits signals attributable to (TPP)-Fe(C_6H_5)(NO) as well as resonance signals at 78.67, 13.3–12.3, and 5.91 ppm, all of which are characteristic of a high-spin iron(III) species. An ESR spectrum with axial symmetry ($g_\perp$ = 5.98 and $g_\parallel$ = 2.00) confirms the existence of a high-spin $S = {}^5/_2$ state in the mixture. Also, UV–visible spectroscopy indicates that no phenyl axial ligand is present in the molecular structure of this compound. This result is consistent with results in the literature.[37]

Electrochemistry of (TPP)Fe(C_6H_5)(NO) and (OEP)Fe-(C_6H_5)(NO). Typical cyclic voltammograms for the oxidation of (TPP)Fe(C_6H_5) and (OEP)Fe(C_6H_5) in PhCN (0.1 M TBA-(PF_6)) in the absence of NO gas are shown in Figures 4 and 5. Oxidation potentials for these complexes are listed in Table VI and match those reported in the literature.[36] Small amounts of NO gas were then added to the initial solution. The NO concentration was monitored by the overall pressure in the vacuum cell. This pressure is proportional to the NO partial pressure since PhCN is a very low vapor pressure solvent (~1 mmHg at 23 °C).

When the NO pressure was increased, peak currents for the first oxidation of (TPP)Fe(C_6H_5) or (OEP)Fe(C_6H_5) decreased in intensity and new waves were obtained at $E_{1/2}$ = 0.86 and 0.73 V for the TPP and the OEP derivatives, respectively. New peaks also appeared at higher pressures of NO and corresponded to oxidations and reductions associated with (P)Fe$(NO)_2$ and (P)-Fe(NO). This is presented in Figure 4 for the case of (TPP)-Fe(C_6H_5) and Figure 5 for the case of (OEP)Fe(C_6H_5).

The initial shift of potentials upon addition of NO gas to (P)Fe(C_6H_5) is consistent with the formation of (P)Fe(C_6H_5)(NO) in solution. This conversion is complete at 72 mm of NO for 1.09×10^{-3} M (TPP)Fe(C_6H_5) (see Figure 4) and 200 mm of NO for 1.31×10^{-3} M (OEP)Fe(C_6H_5) (see Figure 5). The conversion of (P)Fe(R) to (P)Fe(R)(NO) is also illustrated by differential pulse voltammograms recorded during oxidation and reduction under low NO pressures (Figure 6). For the case of (TPP)Fe-(C_6H_5), complete conversion to (TPP)Fe(C_6H_5)(NO) occurs at 72 mm and no evidence of dinitrosyl complexes or NO reduction at negative potentials is evident. This is not the case for the (OEP)Fe(C_6H_5) complex (Figure 6b). At high NO pressure, oxidation of (OEP)Fe$(NO)_2$ is observed at E_{pa} = 0.95 V and reduction of NO (at E_{pc} = −1.20 V) is also measured.

The spectra of (TPP)Fe(C_6H_5) in the presence and absence of NO are illustrated in Figure 2. As seen in this figure, the spectrum of (TPP)Fe(C_6H_5)(NO) in PhCN (0.1 M TBA(PF_6))

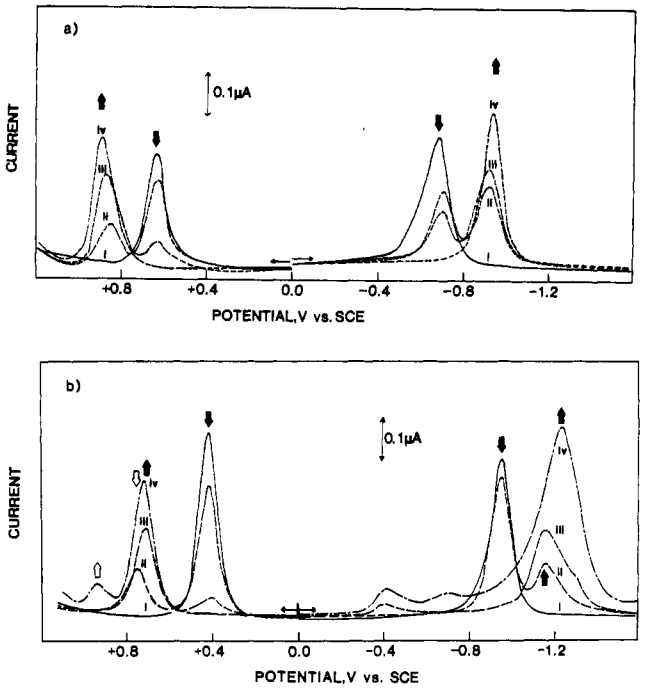

Figure 6. Differential pulse voltammograms of (P)Fe(C_6H_5) under various NO pressures in PhCN (0.1 M TBA(PF_6)): (a) 1.09×10^{-3} M (TPP)Fe(C_6H_5) under NO pressures of (i) 0, (ii) 29, (iii) 48, and (iv) 72 mm; (b) 1.31×10^{-3} M (OEP)Fe(C_6H_5) under NO pressures of (i) 0, (ii) 100, (iii) 200, and (iv) 400 nm.

is relatively close to the one measured in toluene (Table V). Thus, on the basis of these data, the electrooxidation at 0.86 V (for the TPP derivative) and 0.73 V (for the OEP derivative) can be written as

$$(P)Fe(C_6H_5)(NO) \rightleftarrows [(P)Fe(C_6H_5)(NO)]^+ + e^- \quad (2)$$

The mechanism for oxidation of (TPP)Fe(C_6H_5)(NO) and (OEP)Fe(C_6H_5)(NO) at high NO pressures is much less straightforward. At low scan rates (0.10 V/s), (TPP)Fe(C_6H_5)(NO) is oxidized at E_{pa} = 0.92 V to generate [(TPP)Fe$(NO)_2]^+$. These two oxidized species are then reduced at E_{pc} = 0.82 and 0.72 V, respectively. This mechanism was ascertained by multiple-scan cyclic voltammetry at fast scan rates and by cyclic voltammograms initiated at positive potentials. This is shown in Figure 7. In Figure 7a, a rapid scan was initiated at 0.5 V. Under these conditions there is only one reversible electron transfer for oxidation and rereduction. This occurs at $E_{1/2}$ = 0.86 V and is characterized as due to the oxidation of (TPP)Fe(C_6H_5)(NO). A set of coupled oxidation and reduction peaks was also observed on multiple-scan voltammograms as shown by the dashed current–voltage curve in Figure 7. A constant potential of 1.20 V was then applied to the Pt electrode until the current decreased to a constant low value. At this point, a cyclic voltammetric scan was initiated at 1.20 V as shown in Figure 7b. Under these conditions there was only one oxidation wave whose potential corresponded to that for reaction of the dinitrosyl species, (TPP)Fe$(NO)_2$.[37]

Similar electrochemistry was also observed for (OEP)Fe(C_6H_5)(NO) under conditions of high NO pressures. At high NO pressures, two oxidation waves were obtained (at $E_{1/2}$ = 0.73 and 0.95 V). This first wave (see Figure 5) corresponds to the oxidation of (OEP)Fe(C_6H_5)(NO) while the most anodic wave (at E_p = 0.95 V) may be characterized as due to an oxidation of (OEP)Fe$(NO)_2$.[37] The final anodic peak current ratio between the oxidation peak at 0.73 V and that of 0.95 V suggests an approximate 1:1 ratio between the concentrations of the mixed-ligand species and the dinitrosyl species (under 760 mm of NO). However, in this case, care must be taken in relying on only the electrochemical data since the potential for oxidation of (OEP)Fe(C_6H_5)(NO) ($E_{1/2}$ = 0.73 V) is virtually identical with

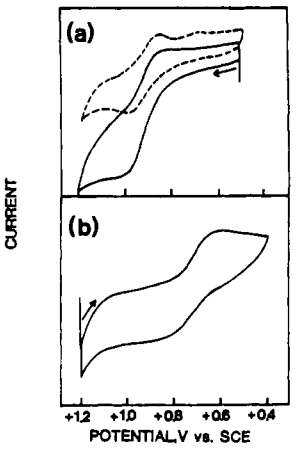

Figure 7. Cyclic voltammograms of 1.09×10^{-3} M (TPP)Fe(C_6H_5)(NO) in PhCN (0.1 M TBA(PF_6)) and under 760 mm of NO: (a) Initial positive scan from 0.5 V (—) and multiscan current–voltage curve after starting at 0.5 V (---); (b) initial negative scan from 1.20 V after holding at this controlled potential for several minutes. The scan rate was 9.9 V/s, and no correction for IR loss was applied.

that for oxidation of (OEP)Fe(NO)($E_{1/2}$ = 0.69 V).

Comparison of Potentials for Oxidation and Reduction of Various σ-Bonded and Nitrosyl-Bonded Fe Porphyrins. The electrochemistry and spectroelectrochemistry of nitrosyliron porphyrins and σ-bonded phenyliron porphyrins has been reported in the literature.[36-38] With the former complexes, the air-stable species contains Fe(II), which (depending on the porphyrin ring) is oxidized to Fe(III) in a range of potential between 0.60 and 0.80 V vs. SCE. For the specific case of (TPP)Fe(NO) in benzonitrile, oxidation of Fe(II) to Fe(III) occurs at 0.75 V.[37] In contrast, σ-bonded alkyl- or aryliron porphyrins contain Fe(III) in the air-stable form. These complexes may be reduced to Fe(II) in the range −0.70 to −1.00 V depending on the porphyrin ring basicity and the type of bound alkyl or aryl group. For the specific case of (TPP)Fe(C_6H_5) in PhCN, reduction to Fe(II) occurs at −0.70 V.[36] An even larger difference of Fe(III)/Fe(II) potentials (1.62 V) is observed for the OEP complexes. In PhCN, (OEP)Fe^{II}(NO) is oxidized at 0.69 V while (OEP)Fe^{III}(C_6H_5) is reduced at −0.93 V.

Addition of pyridine to (P)Fe(R) is also possible and has been studied in detail for the reactions of (OEP)Fe(C_6H_5) and (TPP)Fe(C_6H_5).[38] Stability constants for formation of six-coordinate (P)Fe(R)(py) from (P)Fe(R) are quite low when compared to those for ligation of (P)FeX by pyridine.[39] This is not surprising since the aryl group acts as an electron-donating ligand, thus decreasing the stability of a six-coordinate complex.

Reversible migration of the phenyl group in (P)Fe(R)(py) occurs after electrooxidation, but at high scan rates, reversible oxidations of the Fe(III) complex may be observed.[38] The potentials for these oxidations are negatively shifted with respect to those of the five-coordinate (P)Fe(R) complexes. For example, (TPP)Fe(C_6H_5) is oxidized at 0.61 V in PhCN while (TPP)Fe(C_6H_5)(py) is oxidized at 0.53 V in PhCN containing 1.0 M pyridine and at 0.63 V in neat pyridine. (Large liquid junction potentials exist between neat pyridine and neat PhCN so that care must be taken in making direct comparisons between values of $E_{1/2}$ in those two solvents.)

Similar shifts of reduction potentials are observed upon going from five-coordinate (P)Fe(C_6H_5) to six-coordinate (P)Fe(C_6H_5)(py). For example, (OEP)Fe(C_6H_5) is reduced at −0.93 V in PhCN while (OEP)Fe(C_6H_5)(py) has a reduction potential of −1.03 V in neat pyridine, containing 0.1 M TBA(PF_6).[38] This value is listed in Table VI and is among the most negative potentials ever measured for reduction of a six-coordinate Fe(III) porphyrin.[40]

(38) Lançon, D.; Cocolios, P.; Guilard, R.; Kadish, K. M. *Organometallics* **1984**, *3*, 1164.
(39) Kadish, K. M.; Bottomley, L. A. *Inorg. Chem.* **1980**, *19*, 832.

As shown in this paper, six-coordinate σ-bonded complexes are also formed upon the addition of NO to (P)Fe(R) and a summary of potentials for oxidation and reduction of (OEP)Fe(C_6H_5)(NO) and (TPP)Fe(C_6H_5)(NO) is given in Table VI. This table is organized according to the type of electrode reaction and, for the case of (P)Fe(C_6H_5)(NO), all of the electrode reactions are identified on the basis of an Fe(II) oxidation state for the starting neutral complex. This is consistent with the spectroscopic characterization given in this manuscript.

In summary, the data in Table VI indicate the dramatic effect of the NO group, which stabilizes the Fe(II) oxidation state of (P)Fe(C_6H_5)(NO). This is most evident from the potentials for the Fe(III)/Fe(II) electrode reaction. There is more than a 1.5-V absolute difference in potentials between the electrooxidation and electroreduction of (OEP)Fe(C_6H_5)(NO) and (OEP)Fe(C_6H_5) or between (TPP)Fe(C_6H_5)(NO) and (TPP)Fe(C_6H_5) in the same solvent and supporting electrolyte mixtures. These potential differences are extremely large and indicate that the effect of an NO molecule in stabilizing the iron(II) oxidation state is much greater than that of the σ-bonded phenyl group, which produces an Fe(III) species.

(40) The most negative potential ever measured for reduction of a six-coordinate Fe(III) porphyrin is that for reduction of the negatively charged [(TPP)Fe(F_2)]$^-$. This complex has $E_{pc} = -1.10$ V in Me_2SO.[41]
(41) Bottomley, L. A.; Kadish, K. M. *Inorg. Chem.* **1981**, *20*, 1348.

Acknowledgment. The support of the National Institutes of Health (K.M.K., Grant No. GM25172) is gratefully acknowledged.

Registry No. **1a**, 97704-85-3; **1b**, 97704-86-4; **1c**, 89672-72-0; **1d**, 97704-87-5; **1e**, 89672-73-1; **1f**, 97704-88-6; **2a**, 89672-68-4; **2b**, 97704-89-7; **2c**, 89672-69-5; **2d**, 89672-70-8; **2e**, 89672-71-9; **2f**, 97704-90-0; (OEP)Fe(CH_3), 79197-83-4; (OEP)Fe(*n*-C_4H_9), 79198-01-9; (OEP)Fe(C_6H_5), 83614-06-6; (OEP)Fe(C_6H_4Me-*p*), 83614-08-8; (OEP)Fe(C_6H_4OMe-*p*), 83614-07-7; (OEP)Fe(C_6F_4H), 96482-32-5; (TPP)Fe(CH_3), 79197-95-8; (TPP)Fe(*n*-C_4H_9), 79198-00-8; (TPP)Fe(C_6H_5), 70936-44-6; (TPP)Fe(C_6H_4Me-*p*), 87621-56-5; (TPP)Fe(C_6H_4OMe-*p*), 89673-27-8; (TPP)Fe(C_6F_4H), 96482-33-6; NO, 10102-43-9.

Contribution from the Département de Chimie-Physique de l'Université de Genève, 1211 Genève 4, Switzerland, and Laboratoire de Chimie de Coordination du CNRS associé à l'Université Paul Sabatier, 31400 Toulouse, France

Unusual Paramagnetic Platinum Complexes. An ESR Study of Platinum Blues

PHILIPPE ARRIZABALAGA,*† PAULE CASTAN,*‡ MICHEL GEOFFROY,*† and JEAN-PIERRE LAURENT*‡

Received April 23, 1985

The well-resolved ESR powder spectra of blue platinum complexes prepared from 1-methylhydantoin and 5-methyl-2-pyrrolidinone offer the possibility of probing various structural models. A good agreement between the experimental and the calculated spectra is obtained by assuming that the hyperfine structure is attributed to the coupling of an unpaired electron with four ^{195}Pt nuclei involved in a tetrameric structure.

Introduction

In recent years, a great interest has been raised in a particular area of platinum chemistry, i.e. compounds having a metallic chain and displaying anisotropic properties.[1] This interest has been mainly focused on complexes in which the formal oxidation state of the metal is nonintegral. Partial removal of d_{z^2} electrons (z taken along the mean Pt chain) from the metallic atoms upon oxidation allows substantially improved d_{z^2} orbital overlap and, through a shortening of metal–metal separation, an increased metal–metal interaction. This results in metallic or semimetallic behavior. Independently of the electrical properties of these complexes, which potentially lend themselves to future technologies, a variety of cooperative or localized magnetic properties may be observed. This is seemingly the case for the so-called "platinum blues" for which ESR signals have been reported by Lippert[2] in 1977 and further related by others in more recent works.[3-5] However, these magnetic properties have not been extensively studied, since the main interest paid to these complexes originates from their potential antitumor activity.[6]

The structure of one of these products, the *cis*-diammineplatinum α-pyridone blue, has been fully characterized,[3,7] and comparative studies strongly suggest that all the known amidato blue species are mixed-valent, metal–metal-bonded, and ligand-bridged polymers. Moreover, they exhibit an ESR signal in contrast to the diamagnetic behavior of Pt(II) and Pt(IV) compounds,[4] and therefore, they should be viewed as original materials that may display cooperative properties in connection with electronic delocalization over a number of platinum atoms. However, as the ^{195}Pt hyperfine structure observed with this compound is very poorly resolved, these spectra could never be used to establish definitively the number of platinum atoms involved in these blue complexes. At this stage it may be underlined that ESR signals may also be observed in irradiated platinum complexes[8] but more interestingly in some platinum mixed-valence compounds such as partially oxidized tetracyanoplatinate salts (KCP family), which have been extensively studied.[9,10]

† Université de Genève.
‡ Laboratoire de Chimie de Coordination du CNRS de Toulouse.

(1) See, for example: (a) Robin, M. B.; Day, P. *Adv. Inorg. Chem. Radiochem.* **1967**, *10*, 247–263 and references therein. (b) Miller, J. S.; Epstein, A. J. *Prog. Inorg. Chem.* **1976**, *20*, 1–45. (c) Reis, A. H., Jr.; Peterson, S. W. *Ann. N.Y. Acad. Sci.* **1978**, *313*, 560–579. (d) Miller, J. S. *Ibid.* **1978**, **313**, 25–59.
(2) Lippert, B. *J. Clin. Hemat. Oncol.* **1977**, *7*, 36–42.
(3) Barton, J. K.; Caravana, C.; Lippard, S. J. *J. Am. Chem. Soc.* **1979**, *101*, 7269–7277.
(4) (a) Arrizabalaga, P.; Castan, P.; Laurent, J.-P. *Inorg. Chim. Acta* **1982**, *66*, L9–L11. (b) Neubacher, H.; Zeplatynski, P.; Lohmann, W. *Z. Naturforsch., B: Anorg. Chem., Org. Chem.* **1979**, *34B*, 1015–1018. (c) Seul, M.; Neubacher, H.; Lohmann, W. *Ibid.* **1981**, *36B*, 272–274. (d) Seul, M.; Neubacher, H.; Lohmann, W. *Ibid.* **1981**, *36B*, 651–653. (e) Zaplatynski, P.; Neubacher, P.; Lohmann, W. *Ibid.* **1979**, *34B*, 1466–1467.
(5) Neubacher, H.; Krieger, J.; Zaplatynski, P.; Lohmann, W. *Z. Naturforsch. B: Anorg. Chem., Org. Chem.* **1982**, *37B*, 790–792.
(6) (a) Davidson, P. J.; Faber, P. J.; Fisher, R. G., Jr.; Mansy, S.; Peresie, H. J.; Rosenberg, B.; Van Camp, L. *Cancer Chemother. Rep., Part 1* **1975**, *59*, 287–300. (b) Speer, R. J.; Ridgeway, H.; Hall, L. M.; Steward, D. P.; Howe, K. E.; Lieberman, D. Z.; Newman, A. D.; Hill, J. M. *Ibid. 1975*, *59*, 629–641. (c) Rosenberg, B.; Van Camp, L.; Trosko, J. E.; Mansour, V. H. *Nature (London)* **1969**, *222*, 385–386. (d) Rosenberg, B.; Van Camp, L. *Cancer Res.* **1970**, *30*, 1799. (e) Arrizabalaga, P.; Castan, P.; Laurent, J.-P.; Cros, S.; Francois, G. *Eur. J. Med. Chem.-Chim. Ther.* **1984**, *19*, 501–505.
(7) (a) Barton, J. K.; Rabinowitz, H. N.; Szalda, D. J.; Lippard, S. J. *J. Am. Chem. Soc.* **1977**, *99*, 2827–2829. (b) Barton, J. K.; Szalda, D. J.; Rabinowitz, H. N.; Waszezak, J. W.; Lippard, S. J. *Ibid.* **1979**, *101*, 1434–1441. (c) Barton, J. K.; Best, S. A.; Lippard, S. J.; Walton, R. A. *Ibid.* **1978**, *100*, 3785–3788.
(8) Krigas, S. T.; Rogers, M. T. *J. Chem. Phys.* **1977**, *55*, 3037–3038.

0020-1669/85/1324-3656$01.50/0